Journal of Statistical Physics, Vol. 54, Nos. 5/6, 1989

Analog Simulation of a Simple System with State-Dependent Diffusion

K. Sinha[1] **and Frank Moss**[1]

Received March 30, 1988

We have constructed an electronic simulator of a simple bistable system driven by noise, whose intensity is determined by the instantaneous value of the coordinate. We observe that the most probable state of the system can be reversed by altering the noise intensity only in the neighborhood of the barrier, an effect pointed out by Landauer many years ago in the context of discussions on entropy-related stability criteria for nonequilibrium systems. We compare detailed measurements on the system with the recent white noise calculations of Landauer and van Kampen. The system also has interesting possibilities for tests of contemporary colored noise theory which we illustrate with an example.

KEY WORDS: Simulator; electronic circuit model analog simulator; relative stability; bistability; stability criteria; nonequilibrium systems; colored noise; colored noise theory; multiplicative noise; state-dependent diffusion; reversal of stability; discontinuous noise intensity; path-dependent noise.

1. INTRODUCTION

Many years ago Landauer raised the issue of the implications of state-dependent diffusion in the context of entropy generation and stability in nonequilibrium systems.[1] His point was that the relative stability of a multistable system could be altered by path-dependent diffusion even when localized to the neighborhoods of the potential barriers separating the deterministically stable or metastable modes. That is, the most probable state of such a system cannot be determined from information about the local minima alone. Later it was observed that in certain models, state-dependent diffusion can even generate maxima in the probability distribution at locations where no potential minima exist.[2] These early

[1] Department of Physics, University of Missouri at St. Louis, St. Louis, Missouri 63121.

0022-4715/89/0300-1411$06.00/0

studies gave rise to wide discussions which continue to be of current interest (see, e.g., ref. 3).

The more general problem of diffusion in inhomogeneous media has recently been carefully analyzed by van Kampen.[4] State-dependent diffusion which is periodic and commensurate with a spatially periodic potential can give rise to continuous currents in the absence of externally applied fields. Such systems have recently been treated by Buttiker[5] and van Kampen[6] as well as Landauer.[7]

In this paper we consider the simplest model for state-dependent diffusion in a bistable system as originally suggested.[1] We take the standard quartic as the potential

$$V(x) = -x^2/2 + x^4/4 + \varepsilon x \tag{1a}$$

with the dynamics being determined by the infinitely damped system

$$\dot{x} = x - x^3 + g(x)\,\xi(t) - \varepsilon \tag{1b}$$

where $\xi(t)$ is a Gaussian, white noise with zero mean and correlation $\langle \xi(t)\,\xi(s)\rangle = 2D_n\delta(t-s)$; and where $g(x)$ is defined by

$$\begin{aligned} g(x) &= 1, && \text{for} \quad x < 0 \text{ or } x > 1/2 \\ g(x) &= 1 + \Delta, && \text{for } 0 \leqslant x \leqslant 1/2 \end{aligned} \tag{2}$$

The noise intensity is D_n and ε controls the symmetry of the potential wells. This specific system has recently been analyzed by both van Kampen,[6] who, in a notably clear tutorial, derived the probability densities from thermodynamic arguments as well as from the diffusion equation, and by Landauer.[7]

The effect of the reversal of stability in this bistable system due to an increased temperature (larger D) in the neighborhood of the barrier is illustrated in Fig. 1. Though the illustration is schematic, the graphs are quantitative. On the left is shown $U(x)$ as given by Eq. (1a) with $\varepsilon = 0.05$. On the right are shown the probability densities as measured on the simulator described in Section 3 below for increasing values of Δ. The effect of Δ in reversing the most probable state is clearly evident.

This paper is organized as follows: In Section 2 the theory is briefly reviewed. Expressions for the ratio of the amplitudes of the stationary probability densities in the two wells and for the magnitudes of the discontinuities at the locations where the noise intensity is discontinuously changed are summarized. In Section 3 the simulator and the methods of measurement are described. The main results are presented in Section 4, where measurements of the amplitude ratio of the probability density and the magnitudes of the discontinuities are compared to the theory of refs. 6

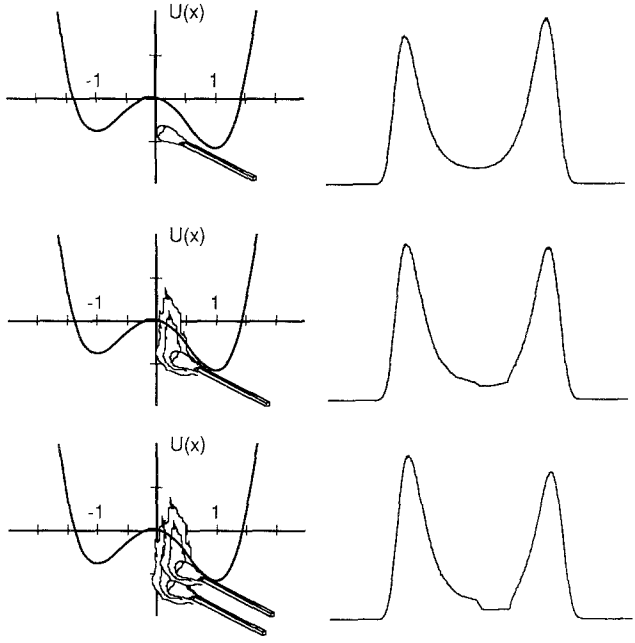

Fig. 1. (Left) Potentials from Eq. (1) with $\varepsilon = 0.05$ and (right) measured densities for $\Delta = 0$, 0.45, and 1.3 (top to bottom), showing the reversal of the most probable state.

and 7. In Section 5 we examine the colored noise problem and the possibility that this system could be of use in the testing of contemporary colored noise theory. As examples, data on the amplitude ratios are compared to the predictions of the conventional small-correlation-time theory, as recently improved by Fox,[8] and to Hanggi's *ansatz*.[9] The advantage of this system is that the results depend only on the *ratios* of probability densities, so that the correlation-time-dependent prefactors which often appear in various forms in colored noise approximate theories *cancel out*, revealing the exponential behavior alone. This could be a considerable advantage, since it is often difficult or impossible to clearly distinguish between the influence of the prefactors and exponentials using numerical, matrix continued fraction, or analog simulations. A vigorous discussion on the merits and accuracy of various colored noise approximate theories is currently in progress.[2] Finally, in Section 6 we summarize our results.

[2] See ref. 10 for a collection of reviews. See also refs. 8, 9, and 11.

2. THEORY

We consider the symmetric potential defined by Eq. (1a) with $\varepsilon = 0$ and as shown in Fig. 2b. Following Landauer's notation,[7] the left-hand well is located at $A\,(x = -1)$, the barrier at $B\,(x = 0)$, the region of increased noise intensity between B and $C\,(x = 1/2)$, and the right-hand well at $D\,(x = 1)$.

It is necessary to first consider what happens at a temperature (or noise intensity) discontinuity. For stationary conditions the probability currents across the discontinuity at B, for example, can be written $\rho(B^-)\,v(B^-) = \rho(B^+)\,v(B^+)$, where ρ is the probability density and v is the

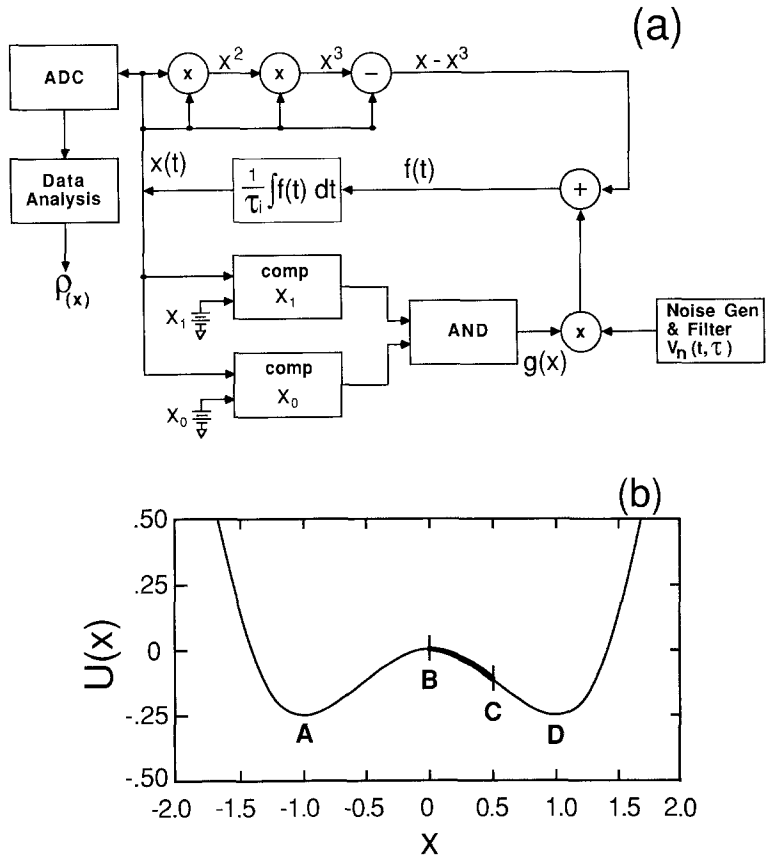

Fig. 2. (a) A schematic diagram of the simulator, showing multipliers (×) summers (±), comparators (comp), and an and circuit (AND). (b) An example of the potential utilized in the simulator with the region of increased noise intensity BC shown in bold lines between $x_0 = 0$ and $x_1 = 1/2$.

velocity of a particle in thermal equilibrium at temperature T just to the left of the discontinuity (B^-) or just to the right (B^+). The velocity is $v \propto T^{1/2}$, so that $\rho(B^+)/\rho(B^-) = (T_L/T_H)^{1/2}$, where T_L is the (lower) temperature outside the region BC and T_H is the (higher) temperature inside BC. We identify the temperature with the diffusion or noise intensity through $D_n = \mu kT$, and since we consider only homogeneous media we take $\mu = \text{const} = 1$. The ratios are thus

$$\rho(B^+)/\rho(B^-) = \rho(C^-)/\rho(C^+) = (D_{nL}/D_{nH})^{1/2} \tag{3}$$

Landauer then argues that the densities within the regions are given by the Boltzmann distribution $\exp[-U(x)/D_n]$. In addition to Eq. (3), the ratios are

$$\rho(B^-)/\rho(A) = \exp[-(U_B - U_A)/D_{nL}]$$
$$\rho(C_-)/\rho(B^+) = \exp[-(U_C - U_B)/D_{nH}]$$
$$\rho(D)/\rho(C^+) = \exp[-(U_D - U_C)/D_{nL}]$$

These probabilities are then multiplied together, whereupon the ratios given by Eq. (3) cancel, and the result is

$$\rho(D)/\rho(A) = \exp[-(U_D - U_A)/D_{nL}] \exp[-\Delta U(D_{nL} - D_{nH})/D_{nL}D_{nH}] \tag{4}$$

where $\Delta U = U_C - U_B$. Van Kampen[6] obtains the same result for the amplitude ratio at the wells, but he predicts for the ratio at the discontinuities

$$\rho(B^+)/\rho(B^-) = \rho(C^-)/\rho(C^+) = D_{nL}/D_{nH} \tag{5}$$

instead of Eq. (3). In this work, we consider only the symmetric ($\varepsilon = 0$) potential. With $U_A = U_D$, Eq. (4) becomes

$$\rho(D)/\rho(A) = \exp[-\Delta U(D_{nL} - D_{nH})/D_{nL}D_{nH}] \tag{6}$$

3. THE SIMULATOR

Figure 2a shows a schematic diagram of the simulator of Eqs. (1) and (2). The design is straightforward and one which we have used before,[9,12] with the exception of the added system for generating $g(x)$. This is shown by the two comparators, which continuously test the voltage on x and compare it to the preset values x_0 and x_1, which mark the boundaries of the region of increased noise intensity. Each time the trajectory crosses of the boundaries an output is applied to the AND gate shown. This gate, in

turn, and the adder which follows it, provide a suitable voltage V_g to a multiplier whose other input is the noise voltage V_n. The logic is arranged in such a way that $V_g = 1 + \Delta$ when $x_0 \leqslant x(t) \leqslant x_1$, and $V_g = 1$ when $x(t)$ is outside this range, or $V_g \equiv g(x)$. The noise voltage $\xi(t)$ which drives the trajectory in the bistable potential is then defined by

$$\xi(t, x) = g(x)\, V_n(t) \tag{7}$$

with $g(x)$ defined by Eqs. (2).

The noise voltage is supplied by a noise generator (Quan Tech model 420) of wide but finite bandwidth, and is therefore necessarily colored. In order to define its correlation time τ_n precisely, it is passed through a linear, single-pole filter with transfer function $H(\omega) = 1/[1 + (\omega\tau_n)^2]$. The simulator scales time with the integrator time constant τ_i, so that the dimensionless correlation time is $\tau = \tau_n/\tau_i$, and the correlation function of V_n is

$$\langle V_n(t)\, V_n(s)\rangle = (D_n/\tau)\exp(-|t-s|/\tau) \tag{8}$$

In the limit $t \to s$, the noise intensity is defined by

$$D_n = \tau\langle V_n^2\rangle \tag{9}$$

and the mean square noise voltage is a measured quantity. In this simulation $\tau_i = 100\ \mu$sec and the range of τ_n was 20–500 μsec (the range of τ was then 0.20–5). For comparison with the white noise theories, however, we set the value $\tau = 0.20$. Equations (2), (7), and (9) then give for the noise intensities

$$D_{nL} = \tau\langle V_n^2\rangle, \qquad D_{nH} = \tau\langle V_n^2\rangle(1+\Delta)^2 \tag{10}$$

Figure 2b shows the potential of Eq. (1a) with $\varepsilon = 0$. The region BC of enhanced noise intensity is shown by the darkened segment which lies between $x_0 = 0$ and $x_1 = 1/2$. The potentials shown in Eq. (4) are then given by $U_A = -1/4$, $U_B = 0$, $U_C = 7/64$, and $U_D = 1/4$, as determined by Eq. (1a) with $\varepsilon = 0$. The theoretical prediction for the amplitude ratio of the densities in the wells, Eq. (4), then becomes

$$\frac{\rho(D)}{\rho(A)} = \exp\left[-\frac{7}{64D_{nL}}\left(1 - \frac{1}{(1+\Delta)^2}\right)\right] \tag{11}$$

Using Eqs. (3) and (10), the predictions for the amplitude ratios at the discontinuities are

$$\rho(B^+)/\rho(B^-) = \rho(C^-)/\rho(C^+) = 1/(1+\Delta) \quad \text{or} \quad 1/(1+\Delta)^2 \tag{12a), (12b)}$$

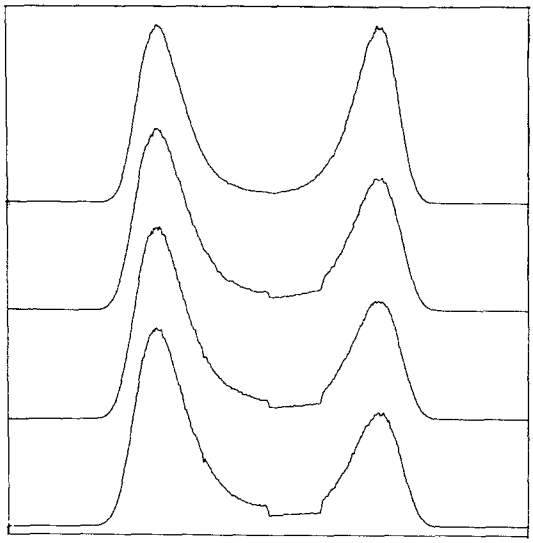

Fig. 3. Probability densities measured for values of $\Delta = 0$, 0.5, 0.75, and 1.0 (top to bottom). The region of increased noise intensity BC is clearly evident for $\Delta > 0$.

The simulator is operated by first setting $\Delta = 0$ and by adjusting ε in order to obtain a symmetric density ρ. Checks on this symmetry adjustment were frequently made throughout the experiment. Figure 3 shows an example set of measured densities for increasing values of Δ, commencing with the symmetric density shown at the top. These densities were assembled as averages from a sequence of time series $x(t)$ of 4096 digitized points each. Typically 800 such time series were obtained, so that each density resulted from about 3.2×10^6 digitized points. For each density, the amplitudes at the two peaks and at the high and low sides of each discontinuity were recorded.

4. THE RESULTS

Figure 4 shows the results of our measurements of the amplitude ratio in the wells as a function of Δ for various values of D_n. The solid lines are plots of Eq. (11) with D_{nL} determined directly from τ and measurements of $\langle V_n^2 \rangle$. There are no adjustable constants. The agreement between Eq. (11) and our measurements is excellent, but probably fortuitous, since the noise driving our simulator is actually colored with $\tau = 0.2$, and the theory is valid only for white noise. The region of quasiwhite behavior of the simulator is $\tau \ll 1$, but in practice the usable dynamic range of the analog

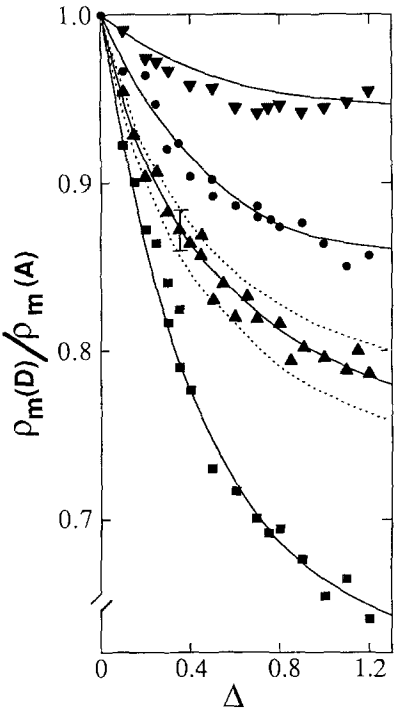

Fig. 4. Plot of $\rho(D)/\rho(A)$ versus Δ for values of $D_{nL}=0.20$ (squares), 0.36 (triangles), 0.60 (circles), and 1.6 (inverted triangles). The solid lines are plots of Eq. (11). The dashed lines estimate the systematic error in D_{nL}.

components imposes a lower limit of $\tau \approx 0.1$–0.2 for reliable operation without voltage clipping. Nevertheless the systematic behavior with D_{nL} and Δ is convincing.

The scatter in the data points shown on Fig. 4 is the result of both systematic and statistical errors. The ratio $\rho(D)/\rho(A)$ is obtained from two large numbers, each with a certain statistical error. The statistical scatter was estimated from short-term repeatability measurements, and is shown as the example error bar on the $D_{nL}=0.36$ data. A more troublesome error stems from longer term variations in $\langle V_n^2 \rangle$ due to very low frequency drifts, or systematic variations, in the noise generator. An attempt has been made to estimate the maximal effects of this error, and is shown by the dashed curves for $D_{nL}=0.40$ (upper curve) and $D_{nL}=0.32$ (lower curve).

We have also measured the amplitudes of the density on both sides of the discontinuities in order to find the ratios $\rho(B^+)/\rho(B^-)$ and $\rho(C^-)/\rho(C^+)$. Both refs. 6 and 7 make specific predictions for the behavior of these ratios with Δ as shown by Eqs. (12). In ref. 7 it is argued

additionally that whatever the functional dependence of the magnitude of the discontinuities on Δ, it can be expected to be the same for both discontinuities, and therefore will cancel in the result Eq. (11). Our measurements of these ratios are shown in Figs. 5a and 5b for a larger and a smaller noise intensity, respectively. The statistical errors on these data are relatively

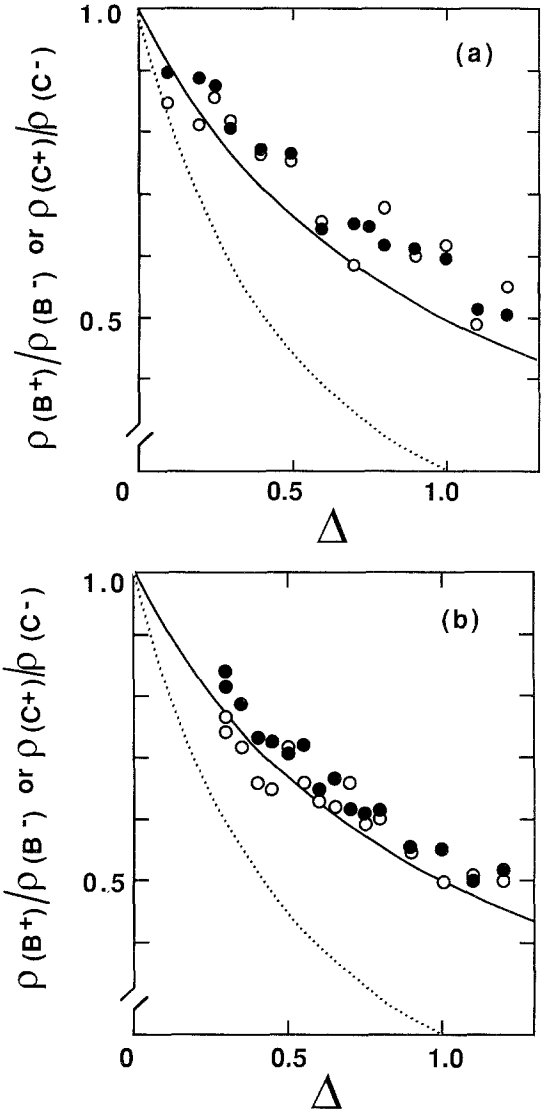

Fig. 5. Plot of $\rho(B^+)/\rho(B^-)$ (solid circles) and $\rho(C^-)/\rho(C^+)$ (open circles) for (a) $D_{nL} = 1.60$ and (b) $D_{nL} = 0.36$. The solid line is Eq. (12a) and the dashed line is Eq. (12b).

larger, as can be judged from the scatter, because the discontinuities occur at low amplitude on the density. The theoretical predictions are shown by the curves: ref. 7 and Eq. (12a) are the solid curves, and ref. 6 and Eq. (12b) are the dashed curves.

We remark that both theories predict the equality of the magnitudes of the two discontinuities and their independence on D. Certainly to within the scatter of our data the measured magnitudes appear to be equal, as shown by the solid circles (discontinuity at B, $x=0$) and the open circles (discontinuity at C, $x=1/2$). Both sets of data seem to lie systematically higher than Eq. (12a), a trend which seems more evident for large noise intensity. Nevertheless, the systematics clearly favors Eq. (12a).

Certainly these results come as no surprise to anyone, since exact solutions of white noise systems in the limit of large damping are very well known. The quasi-white-noise measurements shown here serve to indicate the accuracy of our simulator.

5. COLORED NOISE

Nearly all colored noise approximate theories begin with an effective Fokker–Planck equation

$$\frac{\partial}{\partial t}\rho(x,t)=\frac{\partial}{\partial x}[U'(x)\,\rho(x,t)]+\frac{\partial^2}{\partial x^2}D(x)\,\rho(x,t) \tag{13}$$

wherein the diffusion $D(x)\to D(x,\tau)$ is intended to account approximately for the nonzero point-to-point correlations over x which are induced by a correlated driving force (the colored noise). [The case wherein $D(x)$ is the result of an inhomogeneous *medium* has been recently examined by van Kampen.[4]] The recent rapid growth of the theoretical colored noise industry[8–11] has resulted in a variety of expressions for the "renormalized" diffusion $D(x,\tau)$.

For the purpose of example we choose here only two: the improved "small-τ" approximation of Fox,[8,13] which reduces to the often cited result of Sancho *et al.*[14] in the limit of small τ; and the *ansatz* due to Hanggi.[9] The Fox results are obtained from Eq. (13) with

$$D_{\mathrm{F}}(x,\tau)=D_0[1+\tau U''(x)]^{-1} \tag{14}$$

which results in the stationary density

$$\rho_{\mathrm{F}}(x)=(1-\tau+3x^2\tau)\exp[-U_{\mathrm{F}}(x,\tau)/D_0] \tag{15a}$$

with $U_{\mathrm{F}}(x,\tau)$ for our potential given by

$$U_{\mathrm{F}}(x,\tau)=-x^2/2+x^4/4+\tau(x^2/2-x^4+x^6/2) \tag{15b}$$

Hanggi's results are obtained from Eq. (13) with

$$D_{\mathrm{H}}(x,\tau)=D_0[1+\tau(3\langle x^2\rangle-1)]^{-1} \tag{16}$$

where $\langle x^2\rangle$ is an average over the trajectories, and this $D(x)$ is specific to our potential. The density in this case is

$$\rho_{\mathrm{H}}(x)=N\exp[-U(x)/D_{\mathrm{H}}(x,\tau)] \tag{17}$$

where $U(x)$ is given by Eq. (1a).

As a zeroth-order approximation, we can simply substitute these results into the white noise formula for the ratio of the densities. This procedure is based on the observation that, even though this is a system with state-dependent noise, the space is separated into three regions, within each of which the noise intensity is constant. Nevertheless, simply to substitute colored noise densities for the white ones neglects the effects (if any) of correlations across the boundaries. Our only justification for this procedure is that our measurements of the amplitude ratios of the discontinuities, as discussed below, show no systematic behavior with τ to within our (not so small) statistical errors.

Using Eqs. (15)–(17) results in the predictions

$$\left[\frac{\rho(D)}{\rho(A)}\right]_{\mathrm{F}}=\exp\left[\frac{1}{D_{nL}}\left(1-\frac{1}{(1+\Delta)^2}\right)\left(-\frac{7}{64}+\frac{9\tau}{128}\right)\right] \tag{18}$$

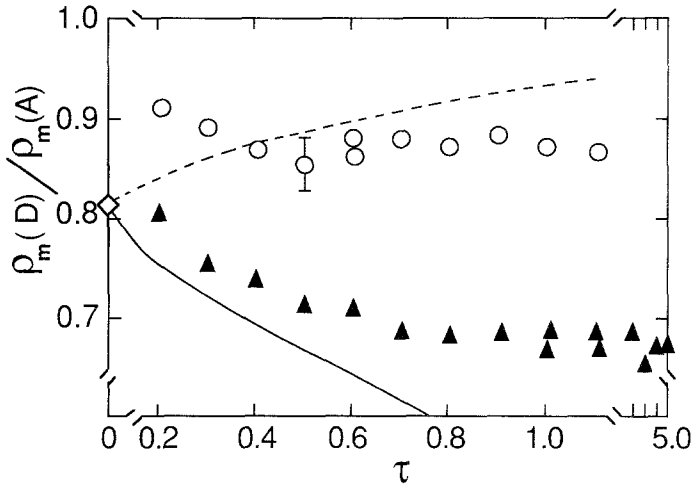

Fig. 6. The effect of colored noise shown by a plot of $\rho(D)/\rho(A)$ versus τ for $\Delta=1$. The open circles are for $D_{nL}=1.6$ and the solid triangles are for $D_{nL}=0.40$. The dashed curve is Eq. (18) and the solid curve is Eq. (19), both for $D_{nL}=0.40$.

for the Fox theory; and

$$\left[\frac{\rho(D)}{\rho(A)}\right]_{\mathrm{H}} = \exp\left[-\frac{7(1+2\tau)}{64D_{nL}}\left(1-\frac{1}{(1+\Delta)^2}\right)\right] \tag{19}$$

for the Hanggi theory. We note that the τ-dependent prefactors (if any) on the densities cancel out in this application. Further, these two expressions make qualitatively opposite predictions: Eq. (18) shows the ratio increasing with τ, while Eq. (19) shows it decreasing. Both show the same Δ dependence (which is also the white noise Δ dependence).

Our measurements at fixed $\Delta = 1$ are shown in Fig. 6, where the open circles are for the large D_{nL} and the solid triangles are for the small D_{nL}. Equation (18) is shown by the dashed curve and Eq. (19) by the solid curve. Both are plotted for $D_{nL} = 0.40$, which is also the noise intensity for which the solid triangles were obtained. The lozenge on the vertical axis shows the white noise limit for all theories and illustrates the difficulty in comparing our simulations with white noise results: the quasi-white-noise simulation was done for $\tau = 0.2$ but does not extrapolate well to the lozenge shown on the axis at $\tau = 0$.

Finally, measurements of the amplitude ratios at the discontinuities versus τ for $\Delta = 1$ are shown in Fig. 7. There is no discernible τ dependence of these ratios.

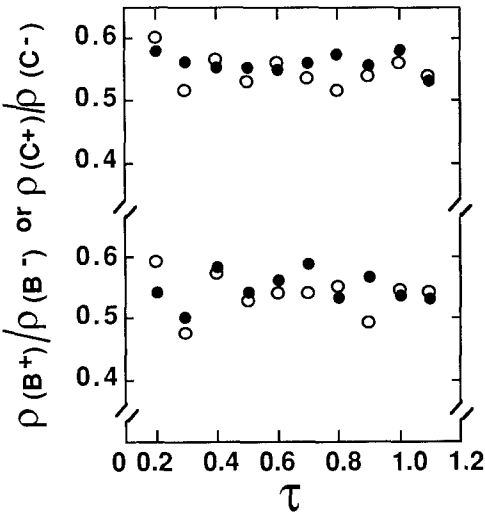

Fig. 7. The effect of noise color τ on the discontinuities $\rho(B^+)/\rho(B^-)$ (solid circles) and $\rho(C^-)/\rho(C^+)$ (open circles). The upper data set is for $D_{nL} = 1.60$ and the lower set for $D_{nL} = 0.40$. All data are for $\Delta = 1$.

6. SUMMARY AND CONCLUSIONS

We have measured stationary density amplitude ratios for a system with state-dependent noise applied in three discrete regions. The noise intensity was changed discontinuously at the boundries of the inner region. The measured results are in good agreement with the predictions of white noise calculations due to Landauer and van Kampen. In addition, we have repeated two sets of amplitude ratio measurements for a range of noise correlation times and compared the results to two current colored noise approximate theories. While neither approximation accurately describes the data, the *ansatz* of ref. 9 is in better qualitative agreement.

ACKNOWLEDGMENTS

We are grateful to R. Landauer and M. Buttiker for stimulating discussions and for suggesting this experiment. We are also indebted to R. Fox, P. Hanggi, and J. M. Sancho for various discussions. This work was supported by the Office of Naval Research, grant N00014-88-K-0084.

REFERENCES

1. R. Landauer, *Phys. Rev. A* **12**:636 (1975); in the *Maximum Entropy Formalism*, R. D. Levine and M. Tribus, eds. (MIT Press, Cambridge, Massachusetts, 1978), p. 321.
2. W. Horsthemke and R. Lefever, *Phys. Lett.* **64A**:19 (1977); *Noise Induced Transitions* (Springer-Verlag, Berlin, 1984).
3. B. J. West and K. Lindenberg, in *Studies in Statistical Mechanics*, Vol. XIII, J. L. Lebowitz, ed. (North-Holland, Amsterdam, 1987), Chapter 2.
4. N. G. van Kampen, *Z. Phys. B* **68**:135 (1987).
5. M. Buttiker, *Z. Phys. B* **68**:161 (1987).
6. N. G. van Kampen, *IBM J. Res. Dev.* **32** (1988).
7. R. Landauer, *J. Stat. Phys.*, to be published.
8. R. Fox, *Phys. Rev. A* **37**:911 (1988).
9. P. Hanggi, T. J. Mrockowski, F. Moss, and P. V. E. McClintock, *Phys. Rev. A* **32**:695 (1985).
10. F. Moss and P. V. E. McClintock, *Noise in Nonlinear Dynamical Systems*, Vol. I (Cambridge University Press, Cambridge, 1988).
11. P. Jung and P. Hanggi, *Phys. Rev. A* **35**:4464 (1987), and preprint; F. Marchesoni, *Phys. Rev. A* **36**:4050 (1987); Th. Leiber, F. Marchesoni, and H. Risken, *Phys. Rev. Lett.* **59**:1381 (1987); J. Masoliver, K. Lindenberg, and B. J. West, *Phys. Rev. A* **35**:3086 (1987); C. R. Doering, P. S. Hagan, and C. D. Levermore, *Phys. Rev. Lett.* **59**:2129 (1987); M. M. Dygas, B. J. Matkowsky, and Z. Schuss, *SIAM J. Appl. Math.*, in press and to be published; S. Faetti and P. Grigolini, *Phys. Rev. A* **36**:441 (1987); L. Schimansky-Geier, *Phys. Lett. A* **126**:455 (1988); V. Altares and G. Nicolis, *J. Stat. Phys.* **46**:191 (1987) and preprint; J. M. Sancho, preprint.
12. F. Moss and P. V. E. McClintock, *Z. Phys. B* **61**:381 (1985).
13. R. F. Fox, *Phys. Rev. A* **33**:467 (1986); **34**:4525 (1986).
14. J. M. Sancho, M. San Miguel, S. L. Katz, and J. D. Gunton, *Phys. Rev. A* **26**:1589 (1982).